Presented at and included in the proceedings of the International Mechanical Engineering Congress and Exhibition in Anaheim, CA, November, 1998. ASME RTD Vol. 15, E.J. Wolf, editor.

ESTIMATION OF RESIDUAL STRESSES IN RAILROAD COMMUTER CAR WHEELS FOLLOWING MANUFACTURE

Jeff Gordon
US Department of Transportation
John A. Volpe National Transportation Systems Center
Cambridge, MA 02142 USA

A. Benjamin Perlman
Department of Mechanical Engineering
Tufts University
Medford, MA 02155 USA

ABSTRACT

A finite element simulation is presented for the prediction of residual stresses resulting from the heat treatment of railroad commuter car wheels during manufacture. The quenching and annealing segments of the wheel manufacturing process are simulated using a decoupled heat transfer and stress analysis. A set of baseline parameters which characterize geometry, material properties and quench characteristics is developed which are representative of current rim-quenching practice. Results indicate the formation of a layer of residual circumferential (hoop) compression to a depth of about 4 cm (1.5 inch) from the tread surface. Variations of these parameters which account for expected ranges in the manufacturing process are shown to have little influence on this finding. The as-manufactured net rim compressive residual stress may be reversed when subjected to service loading in railroad commuter operations. This situation is examined in a companion paper. Tensile stresses at the wheel tread create an environment conducive to the formation of surface cracks that may threaten the safety of train operations. The results of the studies presented in this paper are required to define the initial conditions for analyses of how service conditions may act to change the as-manufactured residual stress state.

INTRODUCTION

In 1991, Federal Railroad Administration (FRA) inspectors became aware of a wheel thermal cracking epidemic in certain New York City area commuter car fleets [1]. Upon investigation of the damaged wheels it was determined that the cracking was caused by thermal fatigue during on-tread friction braking. The thermal cracks appear as short cracks oriented axially on the wheel tread as shown in Figure 1. Figure 2 shows the fracture surface of one of these cracks in which the characteristic beachmarks confirm fatigue as the crack growth driving mechanism.

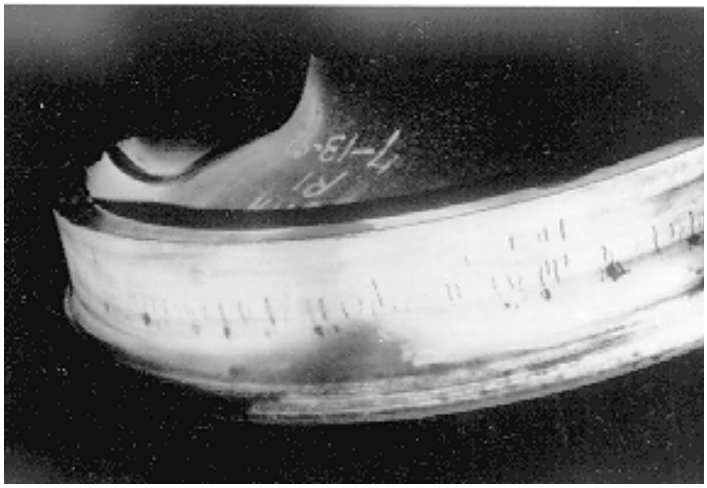

Figure 1. Thermal cracks on commuter wheel tread.

Two of the affected railroads were found to have had brake system maintenance problems which resulted in excessive play in the brake shoe rigging. This led to overhang of the brake shoe and concentration of the frictional heat generated during braking in a narrow band outboard of the center of the wheel tread.

Thermal fatigue due to repeated brake applications from high speed was identified as the primary contributor to the cracking observed in the third fleet. As the operational characteristics of this fleet were the cause of the cracking, wheels in this type of service will be the subject of this investigation and the companion study in which revenue service conditions are simulated [2].

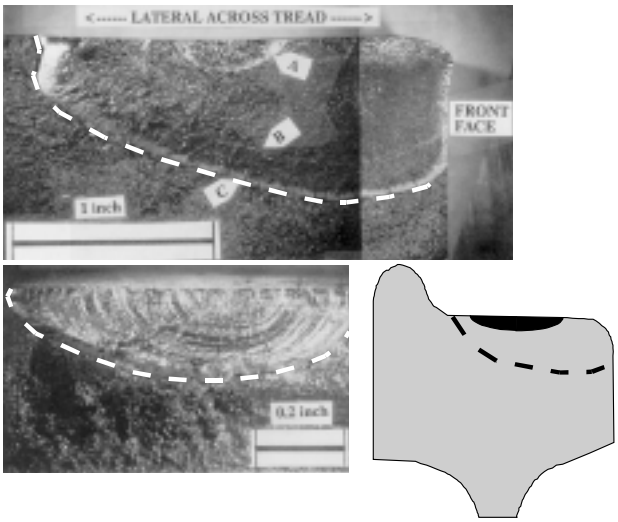

Figure 2. Fatigue crack profile.

WHEEL MANUFACTURING PROCESS

The commuter operations which experienced the thermal cracking problems used the same type of wheels, 32-inch (81 cm) reverse-dish (or S-plate) wheels. A schematic of the wheel cross-section is shown in Figure 3. The S-plate is used in applications in which high-performance stop braking is required in service. The curved plate acts like a spring and permits radial breathing of the rim when it is heated during friction braking. This action reduces the thermal stresses developed in the rim of the wheel.

These wrought wheels are supplied by several vendors in the United States. The wheels are manufactured using a multi-step forging process to initially shape the wheel. Next, to remove undesired residual stresses which remain after forging, they are reheated to a temperature above the austenitizing temperature (*Af*=871°C or 1600°F in this example). Once reheated, the wheels are rim-quenched using a water spray to produce a fine-grained pearlitic microstructure and induce beneficial circumferential (hoop) residual compressive stress at the tread surface. The residual stress distribution inhibits the formation of fatigue cracks in the rim and also retards the growth of these cracks should they manage to form. Following quenching, the wheels are placed in an annealing furnace for several hours to reduce the levels of residual stress. After this heat-treatment, the wheels are exposed to ambient conditions as they cool to room temperature. The resultant distribution of residual stresses represents the as-manufactured condition of "new" wheels, and is a required component for the assessment of service conditions.

IMPLEMENTATION

A decoupled thermo-mechanical analysis of the quenching process was performed to estimate the as-manufactured residual stress state in the subject commuter car wheels. A two-dimensional axisymmetric model of the wheel cross-section was constructed, as shown in Figure 3. Several grids were developed, with varying element density in the rim area. The mesh chosen for this analysis is shown in Figure 4, which contains 989 nodes and 907 quadrilateral elements. The portion of the model not shown is identical to that in Figure 3. A transient heat transfer analysis is conducted to obtain the time history of the temperature distribution in the cross-section. The thermal distributions are used as loads for the stress analysis.

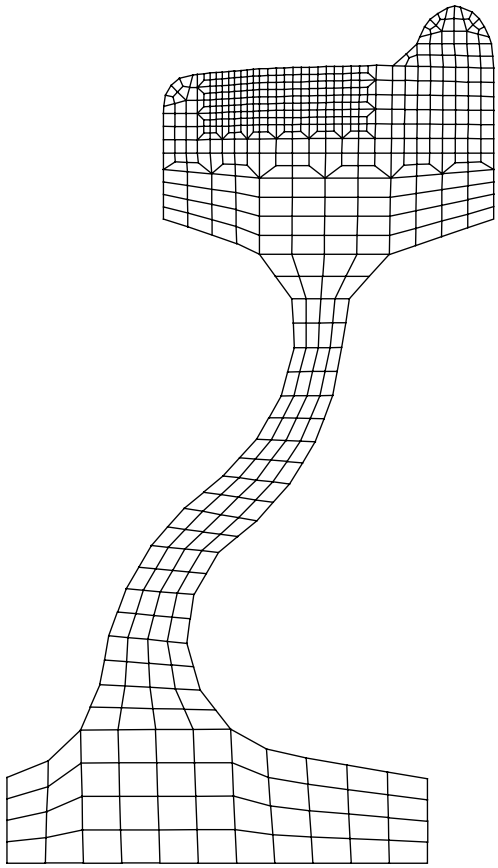

Figure 3. Finite element mesh for quenching simulation.

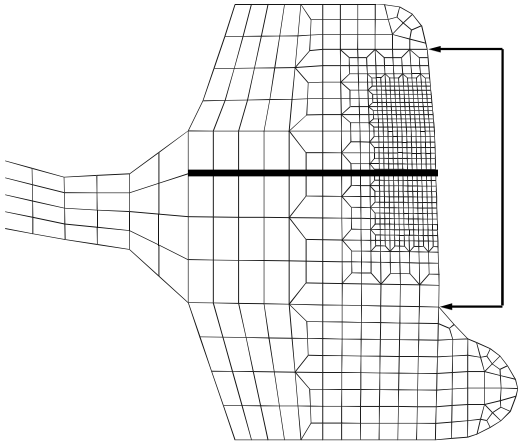

Figure 4. Detail of wheel rim finite element mesh.

THERMAL MODEL DESCRIPTION

ABAQUS/Standard, a commercial implicit finite element computer code [3] was used for the thermal and mechanical analyses. The transient heat transfer analysis begins at the point when the wheel is removed from the austentizing furnace. The water spray quench is applied to the tread surface (the region between the arrowheads in Figure 4) for two minutes, followed by a four-minute dwell at room temperature. Next the wheel enters the annealing furnace at 500°C (932 °F) for a period of five hours. The final step in the process involves air-cooling the wheel to room temperature, which requires about six hours. The process is illustrated schematically in Figure 5.

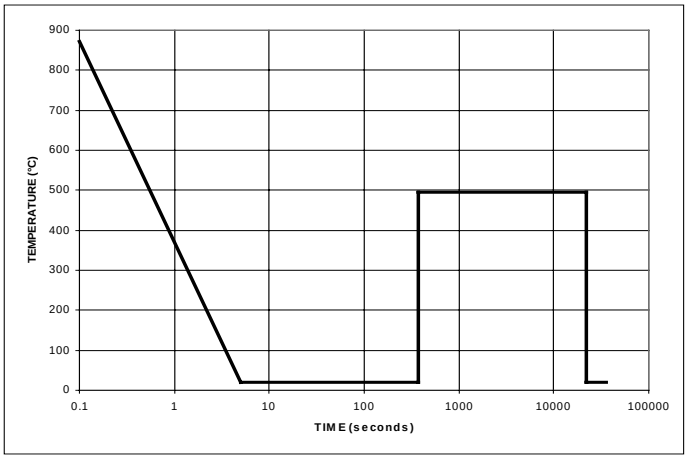

Figure 5. Schematic representation of wheel quenching process: ambient temperature (°C) vs. time (seconds).

Table 1. Material properties for heat transfer analysis.

Temperature (°C)	Specific Heat c_p (J/kg K or °C)	Thermal Conductivity λ (W/m K or °C)
0	419.5	59.71
350	629.5	40.88
703	744.5	30.21
704	652.9	30.18
710	653.2	30.00
800	657.7	25.00
950	665.2	27.05
1200	677.3	30.46

Conduct of the heat transfer analysis requires specification of several material properties which are dependent upon temperature, as defined in Table 1 [4]. The heat transfer coefficients, *h*, between the wheel and its surroundings correspond to values used in a similar analysis for freight wheels and have been obtained from laboratory measurements [5]. During the quench, *h* has a value of 3066 W/m^2 (3.75 Btu/hr in^2 °F) at the tread and 28 W/m^2 (0.0347 Btu/hr in^2 °F) everywhere else. During the rest of the process, *h* has a constant value of 28 W/m^2 (0.0347 Btu/hr in^2 °F) on all exposed wheel surfaces. The heat transfer between the wheel and its support is approximated assuming that the back rim face is in contact with some type of runout table, presumably made of steel. An effective heat transfer coefficient is determined which is related to the contact area and the thermal conductivity of the table, and its magnitude is about half that of the thermal conductivity assumed for the wheel material. Radiation is accounted for assuming a constant value of surface emissivity, ε = 0.95, for all surfaces.

MECHANICAL MODEL DESCRIPTION

Using the same finite element mesh which was used for the heat transfer analysis, the residual stresses in the wheel due to the simulated manufacturing process are estimated. The transient temperature field determined during the heat transfer analysis becomes the time-dependent loading for the mechanical analysis. Additional material properties are required for this aspect of the calculation, and these are listed in Table 2 [4]. The wheel material is assumed to be elastic-plastic with kinematic hardening, as in other investigations. The software employed for this analysis requires specification of the *secant* coefficient of thermal expansion (CTE). This is an important detail, as the magnitude of the secant CTE is related to a reference (initial) temperature. Details on the procedure for conversion of CTE data are presented in [4].

As previous research [5] has identified creep as an important consideration in such simulations, provisions have been made to include this effect in the current work. Viscoelastic creep can be used to represent a stress relaxation phenomenon which occurs in a stressed body which is held at elevated temperature for an extended period of time. This situation occurs during the annealing portion of the manufacturing process and is accounted for in the modeling effort through specification of creep strain rates which are dependent upon the local values of temperature and stress. The creep strain rate is determined from the following equation,

$$\dot{\varepsilon} = 4.64 \cdot 10^{-08} \left(\sigma_{eff}{}^{12.5}\right) e^{\frac{-53712}{T+460}}$$

in which T is the temperature in Fahrenheit and σ_{eff} is the Mises effective stress in ksi (1 ksi = 6.895 MPa) [5]. This equation has been developed from experimental data and appropriate corrections have been made to ensure consistent engineering units [6]. The estimated creep strains are obtained from the calculated strain rates over a small time interval in the calculation.

Table 2. Material properties for stress analysis.

Temp. (°C)	Young's Modulus E (MPa)	Poisson's Ratio ν	Secant CTE α_s $\times 10^{-5}$ at T_{ref} 27°C	Secant CTE α_s $\times 10^{-5}$ at T_{ref} 871°C	Yield Strength σ_{YS} (MPa)	Tangent Modulus E^p (MPa)
24	213	0.295	5.36	9.89	422.9	21.66
230	201	0.307	7.11	10.82	424.7	25.73
358	193	0.314	8.05	11.15	366.7	20.29
452	172	0.320	8.61	11.27	291.0	14.89
567	102	0.326	9.16	11.31	132.3	5.93
704	50	0.334	9.60	11.28	39.4	0.92
900	43	0.345	9.97	11.25	11.7	0.085

RESULTS AND DISCUSSION

The heat transfer analysis yields the time-dependent temperature field which causes the development of the residual stresses, the target of the study. Since the temperature varies with location and time, model results are presented along a path through the rim as shown in Figure 4 (heavy line segment).

Figure 6 shows the temperature distribution through the wheel rim at the end of the two-minute quench along the line shown in Figure 4. The vertical axis represents the depth below the tread surface in cm, and the horizontal axis is the temperature in Celsius. The surface temperature is on the order of 225 °C at the end of the quench. Deeper into the rim the temperature is nearly 800 °C, and differs little from the initial austenitizing temperature (871 °C). The steep thermal gradient in the rim at this time, evident in the contour plot in Figure 7, is the source of the residual stresses which are present at the end of the process. The lighter colors represent lower temperatures (in Celsius) and highlight the progression of the cold front into the rim during the quench. Figure 8 shows the variation of the hoop stress in the rim at the end of the quench as a result of the thermal gradient. The vertical axis in Figure 8 again denotes depth beneath the tread (in cm) and the horizontal axis is hoop stress (in MPa; 6.895 MPa = 1 ksi).

Figures 9 and 10 show the hoop stress evolution during the entire process at two points in the rim, corresponding approximately to the endpoints of the heavy line segment in Figure 4. Figure 9 illustrates the time history for the first 500 seconds during which the most dramatic variations occur due to the progression of the cold front from the quenched surface deeper into the bulk of the rim. Figure 10 shows the evolution of the hoop stress for the entire process. The effect of creep relaxation during the five-hour period while the wheel is in the annealing furnace is evident. Creep accounts for the gradual reduction (in magnitude) of the compression at the surface and the tension deeper into the rim during the interval between 400 and 22,000 seconds as shown in Figure 10.

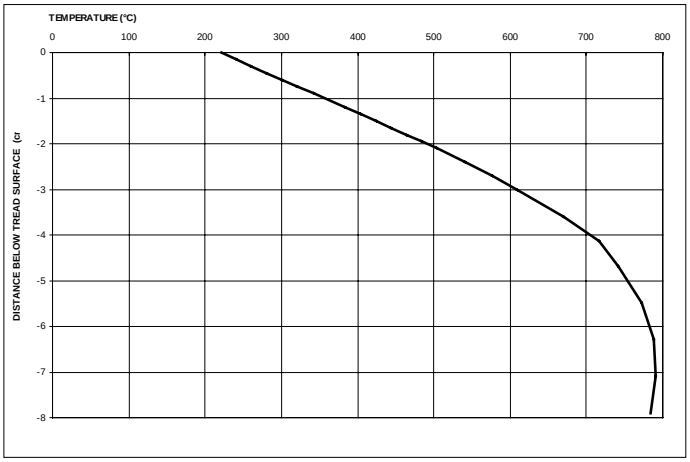

Figure 6. Temperature distribution along line through rim at end of quench (time =125 seconds).

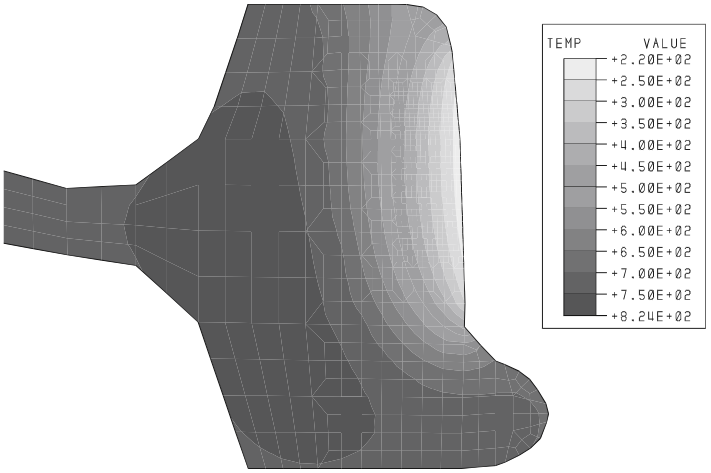

Figure 7. Temperature distribution in wheel rim at end of quench (time=125 seconds).

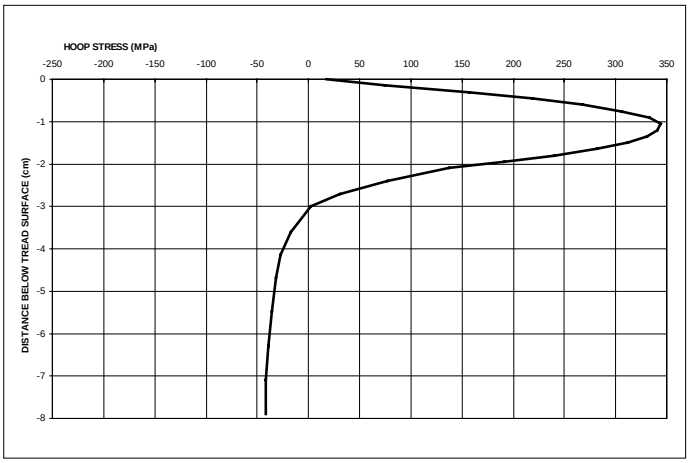

Figure 8. Hoop stress distribution in wheel rim at end of quench (time=125 seconds).

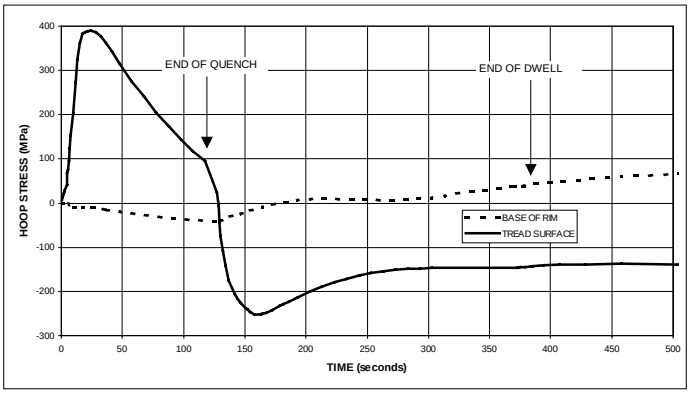

Figure 9. Time history of hoop stress in two rim elements during first 500 seconds of heat treatment..

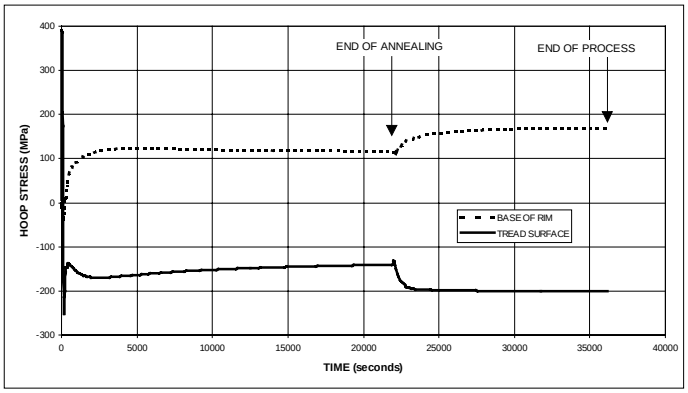

Figure 10. Time history of hoop stress in two rim elements during entire heat treatment.

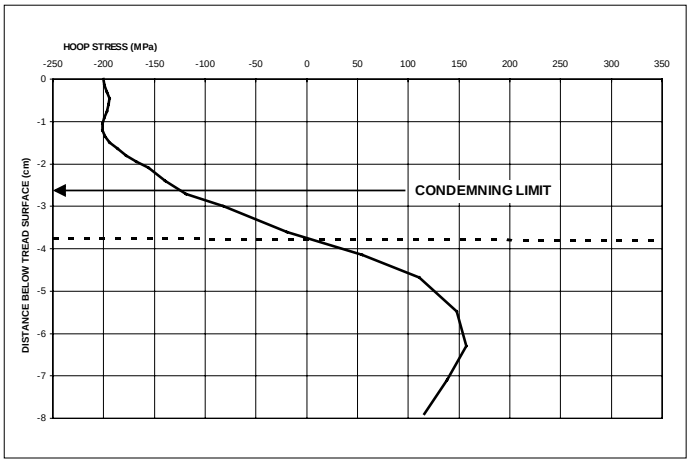

Figure 11. Hoop stress distribution in wheel rim at end of process (time=10 hours).

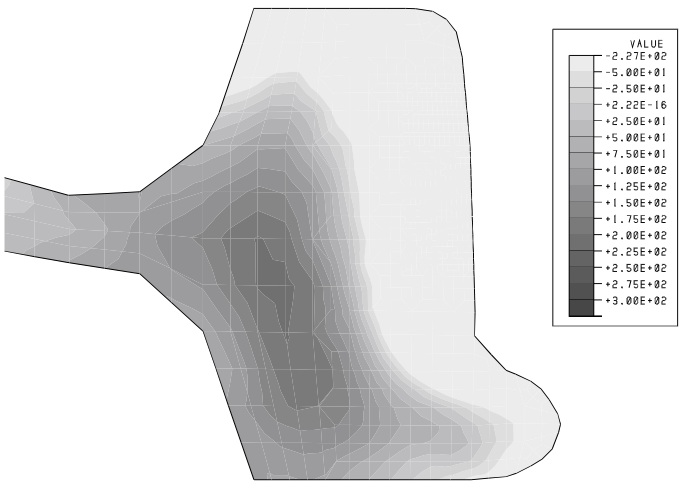

Figure 12. Contours of hoop stress in wheel rim at end of process (time=10 hours).

Figure 11 is a plot through the rim (along the heavy line depicted in Figure 4) of the hoop component of residual stress at the end of the simulated manufacturing process. The heavy dashed line in Figure 11 identifies the boundary between compression and tension and indicates that following manufacturing, the rim is left in residual compression to a depth of about 3.8 cm (1.5 inch). The compressive stress at the surface is on the order of 200 MPa (29 ksi). Figure 11 also identifies the condemning limit, the point to which the wheels may wear before they must be scrapped, and shows that in the absence of any other influences, the wheels will retain residual compression at the tread surface, although at a lower level (125 MPa or 18 ksi).

Figure 12 is a contour plot of hoop stress (in MPa) in the rim at the end of the process. This Figure clearly indicates the compressive region near the tread (the lighter colored contours) and the tension which exists below the compressive layer (the darker contours).

This analysis represents a set of manufacturing variables which are assumed to represent a technical baseline. In order to assess the importance of the various manufacturing process parameters, variations on the baseline conditions were selected to determine the influence of each on the character of the predicted residual stresses at the end of the simulated process. Table 3 lists the options examined and the maximum hoop residual stress on the tread surface (MAX σ_θ) and the depth of penetration of the compressive layer (DEPTH) for each of these variants.

Table 3. Quench model variations.

DESCRIPTION	MAX σ_θ, MPa (ksi)	DEPTH, cm (inch)
Represents the best estimate possible of the manufacturing conditions as well as temperature-dependent material properties with information available.	-200 (-29)	3.75 (1.48)
Baseline conditions with the effects of viscoelastic creep excluded.	-326 (-47)	3.60 (1.42)
Baseline conditions with the duration of the quench extended by 1 minute.	-205 (-30)	4.00 (1.57)
Baseline conditions with the duration of the quench reduced by 1 minute.	-195 (-28)	3.40 (1.34)
Baseline conditions with the annealing temperature increased by 150 °C.	-243 (-35)	3.75 (1.48)
Baseline conditions with the annealing temperature reduced by 150 °C.	-261 (-38)	3.75 (1.48)
Baseline conditions with coefficient of thermal expansion modified to represent the average value of data obtained from other sources.	-208 (-30)	3.90 (1.55)

Figure 13 shows a plot of the data in Table 3 and highlights the relative lack of variation in the predicted residual compressive stress in the rim. In spite of the differences in the simulated manufacturing parameters there is little difference in the predicted depth of the compressive layer or the magnitude of the residual stress at the tread surface. One exception is the result obtained from the analysis in which the effects of creep are excluded. In this case, the depth of the compressive layer is comparable to the other cases, however the magnitude is significantly greater. This result confirms other research

in which the importance of accounting for creep behavior was identified [5].

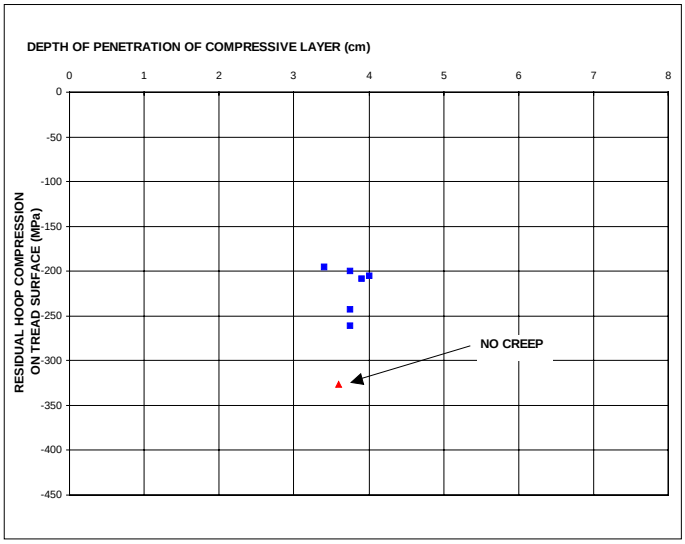

Figure 13. Relationship between magnitude of residual compression at tread surface and depth of penetration of compressive layer.

CONCLUSIONS

A finite element model of the quenching and annealing portions of the manufacturing process of commuter car wheels is presented. Baseline quenching parameters are chosen which are believed to reasonably represent current manufacturing processes. Results of the baseline analysis suggest the presence of a 4 cm (1.5 inch) thick residual compressive layer with stresses as high as 200 MPa (29 ksi) in a new wheel. Variations of the baseline parameters indicate little change in the predicted residual hoop stress in the subject wheels. This insensitivity is fortunate, as it permits exploitation of the model without requiring in-depth knowledge of the manufacturing process, the details of which are often proprietary. The predicted residual stresses resulting from the simulated manufacturing process agree qualitatively with estimates made by other researchers. The estimates of residual stress in the wheel rim developed here represent a rational baseline for characterizing the as-manufactured condition. This as-manufactured state represents the initial condition for a follow-on study which will examine the effects of service conditions (contact loading and thermal stresses from on-tread friction braking) [2].

ACKNOWLEDGMENT

This work was carried out under the Rail Equipment Safety program sponsored by the Office of Research and Development, Federal Railroad Administration, under the direction of Ms. Claire L. Orth, Chief, Equipment and Operating Practices Research Division. Ms. Monique Stewart is the Project Manager for the work related to railroad wheels.

REFERENCES

[1] Orringer, O., Gray, D.E. and McCown, R.J., "Evaluation of Immediate Actions Taken to Deal with Cracking Problems in Wheels of Rail Commuter Cars," Final Report, July, 1993. DOT/FRA/ORD-93/15.

[2] Gordon, J., Jones, J.A., and Perlman, A.B., "Evaluation of Service-Induced Residual Stresses in Railroad Commuter Car Wheels," ASME IMECE RTD, November 1998 (in these proceedings).

[3] Abaqus/Standard User's Manual, Volume I and II (version 5.6). Hibbitt, Karlsson and Sorenson, Inc., Warwick, RI, 1996.

[4] Gordon, J., "Estimation of Residual Stresses in Railroad Car Wheels Resulting from Manufacture and Service Loading," MS Thesis, Department of Mechanical Engineering, Tufts University, February, 1998.

[5] Kuhlman, C., Sehitoglu, H. and Gallagher, M., "The Significance of Material Properties on Stresses Developed During Quenching of Railroad Wheels," Proc. Joint ASME/IEEE Railroad Conference, April, 1988, pp. 55-63.

[6] Sehitoglu, H. and Morrow, J., "Characterization of Thermo-Mechanical Fatigue," ASME PVP., 1983, Vol. 71, pp. 93-100.